

# Formation and electrochemical desorption of self-assembled monolayers as studied by ToF-SIMS

Michal Tencer,<sup>a,b\*</sup> Heng-Yong Nie<sup>c</sup> and Pierre Berini<sup>a,d</sup>

**Time-of-flight secondary ion mass spectrometry (ToF-SIMS) was used to study a number of processes involving thiol-based self-assembled monolayers (SAMs) on nontextured (polycrystalline) gold (Au) films deposited on Si wafers. ToF-SIMS turned out to be a convenient and versatile semiquantitative technique which readily verified electrochemical desorption of a SAM and formation of another SAM on the same sample via reincubation with another thiol. The technique, allowing one to follow simultaneously more than one species on the surface, showed that any formation of a mixed SAM on surfaces which did not undergo electrolysis was negligible with the applied time scale (minutes). Copyright © 2010 John Wiley & Sons, Ltd.**

**Keywords:** thiols; self-assembled monolayer; SIMS; time-of flight; gold; silver; plasmon; polariton; electrolysis; desorption

## Introduction

Thiol-based self-assembled monolayers (SAMs) on gold (Au) surfaces are key elements of the chemical interface needed in biosensors.<sup>[1]</sup> In such sensors, the properties of both the underlying Au as well as those of the self-assembled layer are utilized. Surface plasmon resonance (SPR),<sup>[2–8]</sup> surface enhanced Raman spectroscopy (SERS),<sup>[9]</sup> and long-range surface plasmon polariton (LRSP) waveguides<sup>[10,11]</sup> are all enabled by Au films and applied to biosensors using a thiol-based SAM. SAMs, through chemical modification at their termini, may be rendered promoting or resistant to adsorption of biologically active substances, e.g. protein.<sup>[2,12–15]</sup> High adsorption specificity can be achieved by conjugation of SAMs with appropriate antibodies.<sup>[1,16–18]</sup> For example, plasmonic biosensors implemented using thin Au stripes arranged to form a Mach-Zehnder interferometer (MZI) are of interest.<sup>[10,11]</sup> In this sensor design, the two Au arms are chemically differentiated by depositing different SAMs on each such that the analyte binds selectively to one arm only thus producing a phase shift. Such differentiation can be achieved by selective electrochemical desorption of a SAM from one arm only.<sup>[19,20]</sup> After the selective desorption, the second arm is incubated with another thiol of different properties vs the analyte. During this secondary incubation, not only will the 'clean' arm attain a new SAM layer but also, the formation of a mixed SAM may occur on the other arm. This is, in itself, not necessarily a problem because some mixed SAMs may have better and more selective affinity to the analyte due to reduced steric hindrance,<sup>[21,22]</sup> but one must be able to access, and thus, to control the extent of this process.

Time-of-flight secondary ion mass spectrometry (ToF-SIMS)<sup>[23]</sup> evolved in recent years as a fast semiquantitative tool for surface analysis<sup>[24–26]</sup> which found applications in the area of thiol SAMs on Au,<sup>[25,27–39]</sup> and whose results agree well with other analytical techniques,<sup>[25,29]</sup> and as such, is suitable for the analysis of the composition of mixed SAMs.

The purpose of this work is to develop a ToF-SIMS methodology for following selective gold electrochemical desorption of SAMs

and adsorption of a different thiol forming another SAM which could be used in the process development. Owing to its sensitivity and rich information in detecting ion fragments from the surface of a specimen, ToF-SIMS is especially suited in confirming the completion of electrochemical removal of the existing thiol SAMs as well as the adsorption of the thiol molecules to come. We show that different thiol molecules yield several characteristic ion fragments upon bombardment of the primary ion beam, which allows us access to information as to whether, and/or how, the two types of thiol molecules compete the same Au arm in a MZI.

## Experimental

The 'polycrystalline' or, more appropriately, nontextured Au used was vacuum-evaporated 30-nm-thick Au on 4.5 nm Cr on *p*-type Si wafers. The wafers were cleaved into dies of ~0.5–1 cm<sup>2</sup> surface area. The thiols used in this study were dodecanethiol, HS(CH<sub>2</sub>)<sub>11</sub>CH<sub>3</sub> (≥98%, Arkema Inc.), referred to further in the text as 'DDT' and 11-mercaptoundecyltri(ethylene glycol), HS(CH<sub>2</sub>)<sub>11</sub>(OCH<sub>2</sub>CH<sub>2</sub>)<sub>3</sub>OH (95%, Sigma-Aldrich Canada Ltd), referred to herein as 'TPEG'. Phosphate Buffer (PB) solution 0.1 M, pH = 7.5, was purchased from Sigma-Aldrich Canada Ltd. Deionized water (18 MΩ cm) was prepared in a Zenopure Quatra 90LC machine and 2-Propanol (semiconductor grade, Puranal) was obtained from Riedel-de Haën.

\* Correspondence to: Michal Tencer, University of Ottawa, School of Information Technology and Engineering, 161 Louis Pasteur St., Ottawa, Ontario, K1N 6N5, Canada. E-mail: mtencer@site.uottawa.ca

a University of Ottawa, School of Information Technology and Engineering, 161 Louis Pasteur St., Ottawa, Ontario, K1N 6N5, Canada

b MST Consulting, Ottawa, Ontario, Canada

c Surface Science Western, University of Western Ontario, London, Ontario, N6A 5B7, Canada

d Spectalis Corp., Kanata North RPO, Ottawa, Ontario, K2K 2P4, Canada

The Au surfaces were degreased with 2-propanol, rinsed with deionized water and placed in a Novascan PSD-UV UV-ozone cleaner (5 min UV irradiation followed by 20 min ozone action). To obtain 'pure' SAM specimens, the dies were incubated with 2 mM solution of the appropriate thiol in 2-propanol for 18 h. (The reason of using 2-propanol rather than the commonly used ethanol was non-availability of high purity ethanol due to excise regulations in Canada.) The experiments were carried out at room temperature.

Electrochemical desorption of thiol SAMs from Au surface was performed with a Pine Research AFCBP1 bi-potentiostat using a three-electrode configuration. In order to test the formation of SAMs, measurements of water contact angle on the sample surface were carried out using a VCA Optima, which is described elsewhere.<sup>[20]</sup>

The surface morphology of the bare and thiol SAMs coated Au films were evaluated using the dynamic force mode of a Park Systems XE-100 AFM. A silicon cantilever having a nominal spring constant of 40 N/m and a tip radius of 10 nm was used. In the dynamic force mode, the cantilever was made to vibrate near its resonant frequency (~300 kHz) by a piezo driver. When the tip was within interactive force region with the sample surface, the oscillation amplitude would decrease. Damped amplitude was thus a measure of the tip-sample interaction, which was used as the feedback parameter for the tip to scan (follow) the topographic features of the sample surface. Images of 256 × 256 pixels were collected on an area of 3 μm × 3 μm of the samples to evaluate their surface roughness.

An ION-TOF (Gmbh) TOF-SIMS IV equipped with a Bi liquid metal ion gun was employed to investigate the thiol SAMs on a Au surface. A 25 keV Bi<sub>3</sub><sup>+</sup> cluster primary ion beam with a pulse width of 12 ns (target current of ~1 pA) was used to bombard the sample surface to generate secondary ions from the sample surface. The secondary ions were extracted by an electric field (2 kV), mass separated, and detected via a reflectron-type of time of flight analyzer. The cycle time for the processes of bombardment and detection was 100 μs. A pulsed, low energy (~18 eV) electron flood was used to neutralize sample charging; the current was maintained below ~20 μA maximum to avoid sample damage. The base pressure of analytical chamber was around 1 × 10<sup>-8</sup> mbar. For each sample, spectra were collected from 128 × 128 pixels over an area of 500 μm × 500 μm for 120 s.

## Results and Discussion

Alkanethiol SAMs (especially DDT) on Au have been studied using ToF-SIMS.<sup>[28–34,37–39]</sup> Fragmentation of DDT SAMs on Au provides numerous characteristic ion fragments. However, because TPEG and DDT share a large part of their structure, many characteristic ion fragments for DDT cannot be used to differentiate DDT from TPEG. We need to identify unique ion fragments in order to differentiate the two thiol molecules.

The negative secondary ion mass spectra of pure DDT and pure TPEG SAMs on Au are shown, respectively, in the upper and lower panels of Fig. 1(a)–(g). Spectra were calibrated using H<sup>-</sup>, C<sup>-</sup> and CH<sup>-</sup>. The mass resolution for CH<sup>-</sup> and <sup>34</sup>S<sup>-</sup> was ~4000 and ~6000, respectively. Shown in Fig. 1(a) are spectra from charge/mass (m/z) ratio 12 to 44, from which one can see that TPEG (lower panel) has much stronger O<sup>-</sup> (the measured m/z at the peak centre was 15.995), OH<sup>-</sup> (17.003), CH<sub>3</sub>O<sup>-</sup> (31.020), C<sub>2</sub>HO<sup>-</sup> (41.005) and C<sub>2</sub>H<sub>3</sub>O<sup>-</sup> (43.020) peaks than DDT (upper panel). These oxygen-containing species are fragments from the triethylene glycol

(C<sub>2</sub>H<sub>4</sub>O)<sub>3</sub> group of TPEG. Although these peaks are also seen on the DDT sample, they are much weaker and should be treated as background contamination of the surface (in fact, almost every sample with exposure to air showed these peaks). Also shown in Fig. 1(a) are ion fragments related to sulfur, such as S<sup>-</sup> (31.973) and SH<sup>-</sup> (32.981), as well as hydrocarbons, such as CH<sup>-</sup> (13.008) and C<sub>2</sub>H<sup>-</sup> (25.009), all of which are common for the two thiols.

In order to make use of ToF-SIMS in identifying the two different SAMs, we explored the higher mass fragments which are unique to each thiol. Shown in the lower panel of Fig. 1(b) is a fragment, (C<sub>2</sub>H<sub>4</sub>O)<sub>2</sub>OH<sup>-</sup> (105.061), from the triethylene glycol group, which is characteristic of TPEG. The deprotonated DDT molecular ion fragment, [DDT-H]<sup>-</sup> (or C<sub>12</sub>H<sub>25</sub>S<sup>-</sup>, 201.174), is shown in the upper panel of Fig. 1(c). As shown in the lower panel of Fig. 1(c), adjacent to the characteristic peak of DDT (in the upper panel) is an oxygen-containing peak from TPEG, which is yet to be assigned (even though the mass fits exactly that of C<sub>14</sub>H<sub>17</sub>O). The two peaks are well resolved even though the m/z difference between them is only ~0.04. However, this peak for TPEG does present an interference to that of the [DDT-H]<sup>-</sup>, which should be taken into account when one needs to evaluate the ion intensity of [DDT-H]<sup>-</sup>, for example, as function of incubation time.

We have already shown two characteristic ion fragments, namely those in Fig. 1(b) and (g), for differentiating TPEG from a biotin derivative.<sup>[20]</sup> In this article, we identify more characteristic ion fragments from TPEG to differentiate it from DDT. Shown in the lower panels of Fig. 1(d) and (g), respectively, are a fragment of the TPEG molecule associated with Au atom, [TPEG + Au]<sup>-</sup> (or C<sub>17</sub>H<sub>36</sub>O<sub>4</sub>SAu<sup>-</sup>, 533.229), and the deprotonated TPEG molecule associated with two Au atoms, [TPEG-H + Au<sub>2</sub>]<sup>-</sup> (or C<sub>17</sub>H<sub>35</sub>O<sub>4</sub>SAu<sub>2</sub><sup>-</sup>, 729.193). In the lower panel of Fig. 1(e), there are two fragments of the TPEG molecule associated with Au and S, i.e. [TPEG + AuS]<sup>-</sup> (or C<sub>17</sub>H<sub>36</sub>O<sub>4</sub>S<sub>2</sub>Au<sup>-</sup>, 565.207), and [TPEG + AuSH<sub>2</sub>]<sup>-</sup> (or C<sub>17</sub>H<sub>38</sub>O<sub>4</sub>S<sub>2</sub>Au<sup>-</sup>, 567.196). TPEG has been shown to produce many characteristic ion fragments from the glycol group.<sup>[40,41]</sup> As indicated above, we found that molecular ion fragments of TPEG associated with Au are useful in identifying the molecule.

Shown in the upper panel of Fig. 1(e) is a 'condensation DDT dimer' (i.e. two DDT molecules with a loss of SH<sub>2</sub>) associated with Au, [DDT<sub>2</sub>-SH<sub>2</sub> + Au]<sup>-</sup> (or C<sub>24</sub>H<sub>50</sub>SAu<sup>-</sup>, 567.353), which is 0.157 away from [TPEG + AuSH<sub>2</sub>]<sup>-</sup> as shown in the upper panel. Finally, the upper panel of Fig. 1(f) shows the two characteristic ion fragments of the two different combinations of the deprotonated DDT and Au atom, namely, [DDT-H + Au<sub>2</sub>]<sup>-</sup> (or C<sub>12</sub>H<sub>25</sub>SAu<sub>2</sub><sup>-</sup>, 595.108) and [(DDT-H)<sub>2</sub> + Au]<sup>-</sup> (or C<sub>24</sub>H<sub>50</sub>S<sub>2</sub>Au, 599.324). These Au-associated molecular ion fragments are characteristic for the SAMs of DDT.<sup>[42]</sup>

We have found out that in the positive SIMS, sulfur or molecular ion fragments for any of the thiols are absent. Additionally, none of the negative gold-associate thiol molecular ion fragments as shown above have counterparts in the positive secondary ion spectra. Therefore, in this work, only the negative SIMS were used for identification of the thiols on the surface.

### Electrochemical desorption/postincubation

In this set of experiments four samples of polycrystalline Au films on silicon were investigated; their detailed descriptions are listed and described in Table 1. Static contact angle measurements with DI water were used to estimate the hydrophilicity or hydrophobicity of the samples. The water contact angle on the TPEG SAM ranges 36–40°, reflecting the hydrophilicity of the SAM terminated by

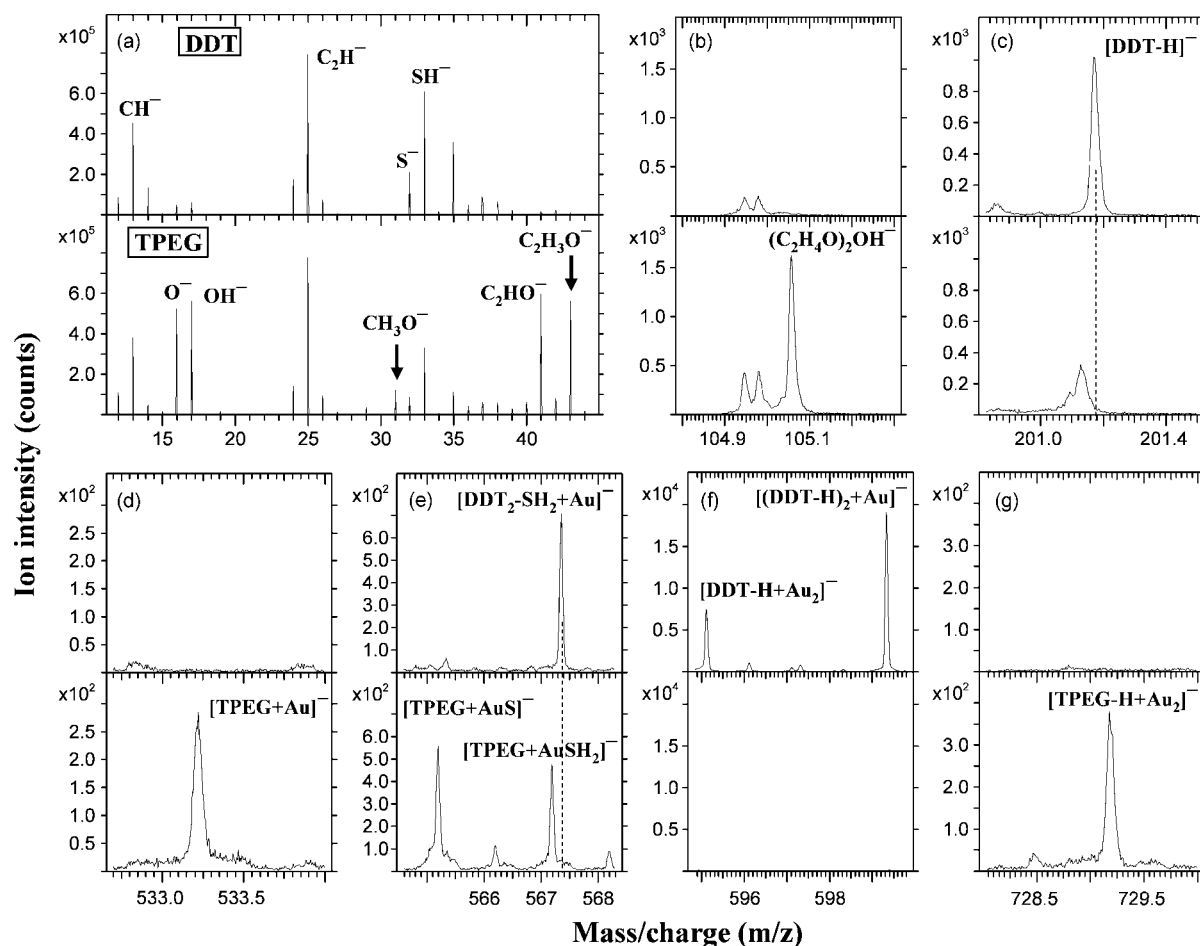


**Figure 1.** Negative secondary ion mass spectra for DDT (upper panel in (a)–(g)) and TPEG (lower panel in (a)–(g)) SAMs on Au. Arrows in (a) and broken lines in (c) and (e) are used to indicate fragments for clarity.

**Table 1.** The electrochemical desorption/postincubation/exchange experiment with water contact angle and RMS surface roughness results

#	Process	Resulting name	Contact angle (°)	Roughness (nm)
1	Overnight incubation of Au film in TPEG solution in isopropanol	TPEG	36–40	0.56
2	TPEG electrolyzed at –2.2 V vs Ag/AgCl	TPEG–2.2 V	46–48	0.46
3	TPEG–2.2 V incubated with DDT solution for 18 h	TPEG–E–DDT	99–103	0.49
4	TPEG incubated with DDT for 18 h	TPEG–DDT	47–54	0.85

hydroxyl groups. After electrochemically removing the TPEG SAM, a slight increase in water contact angle (46–48°) reflects the exposed Au surface of sample TPEG–2.2 V. After the TPEG–2.2 V sample was incubated in the DDT solution for 18 h, DDT SAM

formed, as evidenced by the contact angle (99–103°), reflecting the formation of closely packed, methyl-terminated, DDT SAM on the Au surface. On the other hand, a TPEG SAM sample incubated in DDT solution for 18 h, named TPEG–DDT, showed a slight increase in contact angle 47–54°, which suggests a possible exchange and/or addition of DDT to some extent, but still far from a total exchange.

The root mean square surface roughness shown in Table 1 is estimated from an AFM image collected on an area of 3 μm × 3 μm for each sample. The images for the four samples are shown in Fig. 2 by false colors with brighter areas being higher in height. The surface roughness for samples TPEG, TPEG–2.2 V and TPEG–E–DDT is around 0.5 nm, which is similar to the roughness for a bare Au film. For sample TPEG–DDT the surface roughness is 0.85 nm. However, without counting the protruding particles seen in Fig. 2(d), the surface roughness becomes 0.60 nm. It is thus clear that the processes described in Table 1 do not alter the surface morphology noticeably.

We conducted ToF-SIMS experiments with the four samples described in Table 1 to follow the change in thiol SAMs caused by the electrochemical process as well as the incubation process. The results for some characteristic ion fragments are shown in Fig. 3. From the first panel of Fig. 3(a) and (b), on the TPEG sample, we can see that the TPEG molecule is characterized by the molecular ions associated with single and double Au atoms, [TPEG + Au]<sup>–</sup> and [TPEG–H + Au<sub>2</sub>]<sup>–</sup>. As shown in the second panel of Fig. 3(a)

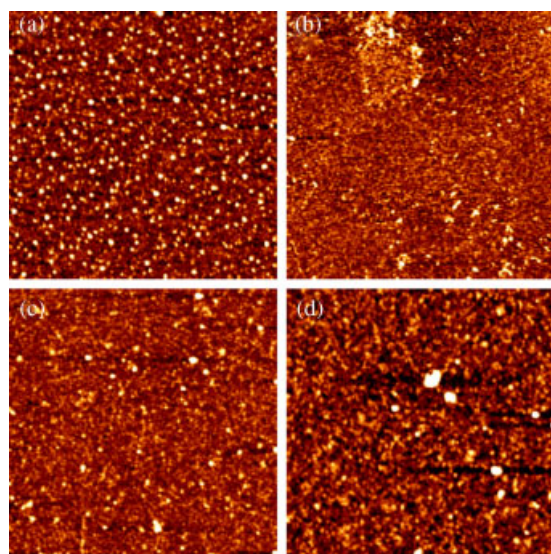


**Figure 2.** AFM topographic images for (a) TPEG, (b) TPEG-2.2 V, (c) TPEG-E-DDT and (d) TPEG-DDT samples. The samples are described in Table 1. The scan area is  $3 \mu\text{m} \times 3 \mu\text{m}$  and the height range (darkest to brightest) is 4 nm.

and (b), after electrolysis at  $-2.2 \text{ V}$  (Ag/AgCl), those characteristic TPEG peaks disappeared completely from the TPEG-2.2 V sample, confirming that the TPEG molecules were removed from the surface by the electrochemical process.

It is also possible to see very weak TPEG peaks on the TPEG-E-DDT sample in the third panel of Fig. 3(a) and (b) which could be a result of small cross-contamination occurring in one of the steps in the process. Figure 3(c) and (d) shows the lack of  $[\text{DDT-H}]^-$ ,  $[\text{DDT-H} + \text{Au}_2]^-$  and  $[(\text{DDT-H})_2 + \text{Au}]^-$  ion fragments for the TPEG SAM sample before (the first panel) and after (the second panel) the electrochemical removal of the TPEG SAMs. After the electrochemical removal of the TPEG SAMs, incubation with DDT solution resulted in formation of DDT SAMs on the Au surface, as identified by  $[\text{DDT-H}]^-$  shown in the third panel in Fig. 3(c) and by  $[\text{DDT-H} + \text{Au}_2]^-$  and  $[(\text{DDT-H})_2 + \text{Au}]^-$  in the third panel in Fig. 3(d).

On sample TPEG-DDT, characteristic TPEG peaks  $[\text{TPEG} + \text{Au}]^-$  and  $[\text{TPEG-H} + \text{Au}_2]^-$  were detected as seen in the last panels of Fig. 3(a) and (b), with reduced intensity in comparison with those from the original TPEG SAM sample (first panel). The decrease of the TPEG ion fragments can be explained by its exchange with the DDT molecules. Indeed, as shown in the last panel in Fig. 3(c) and (d), after the incubation of the TPEG SAM sample in the DDT solution, DDT was identified by  $[\text{DDT-H}]^-$ ,  $[\text{DDT-H} + \text{Au}_2]^-$  and  $[(\text{DDT-H})_2 + \text{Au}]^-$ . In the first panel in Fig. 3(d), a weak peak seen on TPEG cannot be assigned to  $[\text{DDT-H} + \text{Au}_2]^-$ , because there is

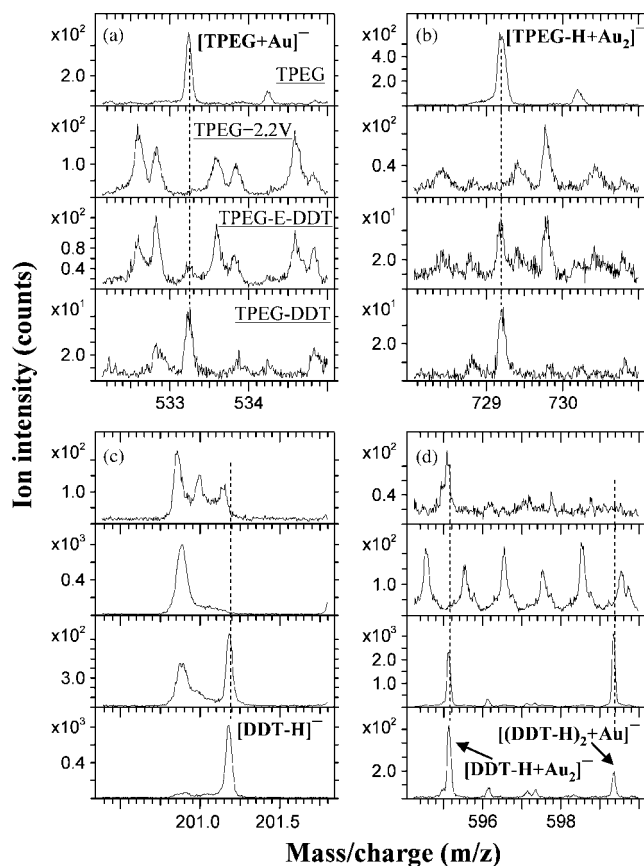


**Figure 3.** Negative secondary ion mass spectra showing characteristic peaks for TPEG (a), (b) and DDT (c), (d) for the processed samples as described in Table 1. Each of the panels in (a) shows the name of the sample from which the spectra were collected; this remains true for (b)–(d). Broken lines in (a)–(d) and arrows in (d) are used for clarity.

no DDT on the TPEG sample as confirmed by the lack of a peak at the position for  $[(\text{DDT}-\text{H})_2 + \text{Au}]^-$ .

As seen above, because multiple characteristic ion fragments for both molecules were identified, ToF-SIMS is a suitable technique for assessing the electrochemical removal and incubation processes. The electrochemical removal of TPEG SAM and formation of DDT SAM was confirmed, as well as a formation of a mixed SAM during an 18 h TPEG/DDT exchange<sup>[43]</sup> and/or addition<sup>[44]</sup> process. The extent to which this exchange/addition takes place is a complex matter involving, for example, possible addition of the thiol molecules in solution to the existing thiol SAMs on the Au surface, possibly further complicated by matrix effects on the ion yields and is currently under investigation.

## Conclusion

We have demonstrated that ToF-SIMS is a powerful analytical technique suited to study of processes involving the formation and removal SAMs on Au surfaces. The technique easily confirmed SAM formation, its electrochemical removal, and the subsequent formation of another SAM in its place. Thus, it is perfectly suitable to any qualitative investigation. Work to develop ToF-SIMS into a quantitative technique to study chemical kinetics and reaction mechanisms in the studied SAM system is in progress, although, obviously, it has to be limited to *ex situ* studies. This involves comparison with other spectroscopic and surface-specific techniques used for such systems<sup>[45]</sup> as well as addressing the technique's possible limitations, e.g. matrix effects.<sup>[46]</sup>

## References

- [1] J. Love, L. A. Estroff, J. K. Kriebel, R. G. Nuzzo, G. M. Whitesides, *Chem. Rev.* **2005**, *105*, 1103.
- [2] V. Silin, H. Weetall, D. J. Vanderah, *J. Coll. Interf. Sci.* **1997**, *185*, 94.
- [3] M. Mrksich, G. B. Sigal, G. M. Whitesides, *Langmuir* **1995**, *11*, 4383.
- [4] J. Homola, S. S. Yee, G. Gauglitz, *Sens. Actuators, B* **1999**, *54*, 3.
- [5] J. Homola, *Chem. Rev.* **2008**, *108*, 462.
- [6] J. Dostálek, A. Kasry, W. Knoll, *Plasmonics* **2007**, *2*, 97.
- [7] M. Vala, S. Etheridge, J. A. Roach, J. Homola, *Sens. Actuators, B* **2009**, *139*, 59.
- [8] A. W. Wark, H. J. Lee, R. M. Corn, *Anal. Chem.* **2005**, *77*, 3904.
- [9] C. T. Nguyen, J. T. Nguyen, S. Rutledge, J. N. Zhang, C. Wang, G. C. Walker, *Cancer Letters*, **2010**, *292*, 91.
- [10] R. Charbonneau, M. Tencer, N. Lahoud, P. Berini, *Sens. Actuators, B* **2008**, *134*, 455.
- [11] M. Tencer, R. Charbonneau, P. Berini, *Lab Chip* **2007**, *7*, 483.
- [12] E. Ostuni, R. G. Chapman, R. E. Holmlin, S. Takayama, G. M. Whitesides, *Langmuir* **2001**, *17*, 5605.
- [13] K. L. Prime, G. M. Whitesides, *J. Am. Chem. Soc.* **1993**, *115*, 10714.
- [14] M. Wanunu, A. Vaskevich, I. Rubinstein, *Isr. J. Chem.* **2005**, *45*, 337.
- [15] A. Sethuraman, M. Han, R. S. Kane, G. Belfort, *Langmuir* **2004**, *20*, 7779.
- [16] S. F. Chen, L. Y. Liu, J. Zhou, S. Y. Jiang, *Langmuir* **2003**, *19*, 2859.
- [17] W.-C. Tsai, I.-C. Li, *Sens. Actuators, B* **2009**, *136*, 8.
- [18] K. Wadu-Mesthrige, N. A. Amro, G.-Y. Liu, *Scanning* **2000**, *22*, 380.
- [19] M. Tencer, P. Berini, *Langmuir* **2008**, *24*, 12097.
- [20] M. Tencer, H.-Y. Nie, P. Berini, *J. Electrochem. Soc.* **2009**, *156*, J386.
- [21] J. Spinke, M. Liley, F.-J. Schmitt, H.-J. Guder, L. Angermaier, W. Knoll, *J. Chem. Phys.* **1993**, *99*, 7012.
- [22] J. Spinke, M. Liley, H.-J. Guder, L. Angermaier, W. Knoll, *Langmuir* **1993**, *9*, 1821.
- [23] A. Benninghoven, *Angew. Chem. Int. Ed.* **1994**, *33*, 1023.
- [24] J. R. Scott, L. S. Baker, W. R. Everett, C. L. Wilkins, I. Fritsch, *Anal. Chem.* **1997**, *69*, 2636.
- [25] D. A. Offord, C. M. John, M. R. Linford, J. H. Griffin, *Langmuir* **1994**, *10*, 883.
- [26] J. T. Francis, H.-Y. Nie, N. S. McIntyre, D. Briggs, *Langmuir* **2006**, *22*, 9244.
- [27] K. V. Wolf, D. A. Cole, S. L. Bernasek, *Anal. Chem.* **2002**, *74*, 5009.
- [28] D. J. Graham, B. D. Ratner, *Langmuir* **2002**, *18*, 5861.
- [29] A. Auditore, N. Tuccitto, S. Quici, G. Marzanni, F. Puntoriero, S. Campagna, A. Licciardello, *App. Surf. Sci.* **2004**, *231–232*, 314.
- [30] S. Sohn, M. Schröder, D. Lipinsky, H. F. Arlinghaus, *Surf. Interface Anal.* **2004**, *36*, 1222.
- [31] L. Xi, Z. Zheng, N.-S. Lam, H.-Y. Nie, O. Grizzi, W. M. Lau, *J. Phys. Chem. C* **2008**, *112*, 12111.
- [32] N. W. Ghonaim, M. Nieradko, L. Xi, H.-Y. Nie, J. T. Francis, O. Grizzi, K. Yeung, W. M. Lau, *Appl. Surf. Sci.* **2008**, *255*, 1029.
- [33] S. N. Patole, C. J. Baddeley, D. O'Hagan, N. V. Richardson, *J. Phys. Chem. C* **2008**, *112*, 13997.
- [34] M. Schröder, S. Sohn, H. F. Arlinghaus, *Appl. Surf. Sci.* **2004**, *231–232*, 164.
- [35] K. Leufgen, M. Mutter, H. Vogel, W. J. Szymczak, *J. Am. Chem. Soc.* **2003**, *125*, 8911.
- [36] F. Cheng, L. J. Gamble, D. G. Castner, *Anal. Chem.* **2008**, *80*, 2564.
- [37] J. H. Wandass, J. A. Gardella, *J. Am. Chem. Soc.* **1985**, *107*, 6192.
- [38] B. Hagenhoff, A. Benninghoven, J. Spinke, M. Liley, W. Knoll, *Langmuir* **1993**, *9*, 1622.
- [39] S. C. C. Wong, N. P. Lockyer, J. C. Vickerman, *Surf. Interface Anal.* **2005**, *37*, 721.
- [40] M. S. Wagner, S. Pasche, D. G. Castner, M. Textor, *Anal. Chem.* **2004**, *76*, 1483.
- [41] H. B. Lu, C. T. Campbell, D. G. Castner, *Langmuir* **2000**, *16*, 1711.
- [42] M. J. Tarlov, J. G. Newman, *Langmuir* **1992**, *8*, 1398.
- [43] C. Chung, M. Lee, *J. Electroanal. Chem.* **1999**, *468*, 91.
- [44] J. Heeg, U. Schubert, F. Kuchenmeister, *Fresenius J. Anal. Chem.* **1999**, *365*, 272.
- [45] D. K. Schwartz, *Ann. Rev. of Phys. Chem.* **2001**, *52*, 107.
- [46] A. V. Walker, *Anal. Chem.* **2008**, *80*, 8865.